deformation-potential constants a', b', and d', similar to the valence-band deformation-potential constants. Since the impurity level is shifted together with the band edge in hydrostatic compression, $a=a'$, which has been experimentally confirmed.[17,20] The results of Bir *et al.*[18] for Ge and Si for the case $\Lambda=\infty$, and measured values of b' and d' for the acceptor-state transition for GaAs (line B) are listed in Table I. The initial slope in the low-stress region is used to obtain b' and d'. The theoretical values for GaAs cannot be computed because the effective-mass parameters have not been determined. The experimental values obtained for GaAs are reasonably close to the theoretical values for Si and Ge. Another theoretical study[21] pertaining to the measurements of peak shift with stress of GaAs *p-n* junction luminescence[22] gave $b'/b=d'/d=0.2$. These values do not fit our data. We observe, in the case of line B, a small difference in the peak energies in the components polarized parallel and perpendicular to the stress direction. The observed effect is inconsistent with the explanation given by Emtage,[21] who attributed the above transitions to the two doubly degenerate states of $J=\frac{3}{2}$ multiplet of the acceptor level.

[20] J. Feinleib, S. Groves, W. Paul, and R. Zallen, Phys. Rev. **131**, 2070 (1963).
[21] P. R. Emtage, J. Appl. Phys. **36**, 1408 (1965).
[22] R. C. Miller, F. M. Ryan, and P. R. Emtage, in *Proceedings of the 7th International Conference on Semiconductor Physics, Paris, 1964* (Academic Press Inc., New York, 1965).

IV. CONCLUSION

We conclude from the study of the stress dependence of the luminescent spectra of GaAs that line A does not involve an acceptor state whereas line B does. Both linear and quadratic stress dependences are used to obtain the deformation-potential constants for the line A. The deformation-potential constants obtained from the linear slope in the low-stress region in the case of an acceptor state are consistent with the theoretical estimate made using valence-band parameters for Ge and Si in the limit of large spin-orbit splitting.[18] More complete comparison of theory and experiment must await determination of valence-band parameters for GaAs.

ACKNOWLEDGMENTS

The authors would like to thank Dr. P. J. Price for stimulating suggestions, Dr. J. C. McGroddy, Dr. W. V. Smith, and Dr. F. Stern for their comments on the manuscript, and J. A. Bradley for invaluable technical assistance.

PHYSICAL REVIEW VOLUME 161, NUMBER 3 15 SEPTEMBER 1967

Irradiation Damage in *n*-Type Germanium at 4.2°K*†

T. A. CALLCOTT‡ AND J. W. MACKAY
Department of Physics, Purdue University, Lafayette, Indiana
(Received 14 November 1966; revised manuscript received 15 May 1967)

The conductivity measured during the application of pulsed electric fields is used to monitor the damage introduced at 4.2°K by energetic electron irradiation of *n*-type germanium. Fields above about 20 V/cm completely ionize the donor impurities. Radiation-induced defects deplete the electron population of the donors by introducing deeper acceptor levels. A sensitivity to defect concentrations of 10^{12} cm^{-3} is obtained in material containing about 10^{14} Sb impurities cm^{-3}. The introduction rates of various defects are studied as a function of irradiation energy. One type, previously identified as a close vacancy-interstitial pair, is removed (presumably by annihilation) in the order of minutes by annealing at 65°K. This defect accounts for 95% of the conductivity change produced by irradiation at 0.7 MeV, but only 50% of the change at 4.5 MeV. Evidently this is the primary defect requiring the least energy for its formation. A second type of primary defect is distinguished by the fact that it is present after annealing to 90°K. The dependence on bombardment energy of the introduction rate of this defect indicates that multiple displacements may be involved in its production, and therefore it may be a double vacancy. A third type of defect is observed only after large fluxes of low-energy electrons, and appears to be a secondary defect resulting from radiation-induced conversion of primary defects. This defect also remains after annealing to 90°K, but it has electrical properties very similar to those of the defect that anneals at 65°K. Trapping properties of the first and third defect types lead to the conclusion that they are both capable of capturing two electrons in *n*-type germanium and are therefore double-acceptor centers.

I. INTRODUCTION

ELECTRICAL measurements provide a very sensitive means of detecting damage centers introduced into germanium by energetic electron irradiation. Radiation defects change the population of carriers by introducing donor or acceptor levels into the forbidden gap. Above about 30°K in lightly doped *n*-type germanium, small changes in carrier concentration due to the introduction of defects with energy levels below the Fermi energy are given by

$$\Delta n=\sum_i \delta_i N_i\,, \quad \Delta n/n_0 \ll 1\,, \tag{1}$$

* This paper is based on a Ph.D. thesis submitted by T. A. Callcott to Purdue University, June 1965.
† Support for this work was provided by U. S. Atomic Energy Commission Contract No. AT(11-1)-125.
‡ Present address: Bell Telephone Laboratories, Murray Hill, New Jersey.

where N_i is the number of the ith type of defect, δ_i their charge in electronic units, and n_0 is the exhaustion range carrier concentration before irradiation. Defect concentrations $N \simeq 10^{12}$ cm^{-3} can be accurately determined by Hall effect and/or conductivity measurements in material with $n_0 \simeq 10^{14}$ cm^{-3}. At liquid-helium temperature, useful dc measurements on such pure material are not possible because conduction electrons are frozen out on the group-V chemical-doping impurities.

Direct-current measurements can be made on degenerate samples with $n_0 \gtrsim 2\times10^{17}$ cm^{-3} even at the lowest temperatures, and give reliable measurements of radiation-defect concentrations of the order of 10^{15} cm^{-3}. Such measurements have shown that thermally induced changes in defect structure occur at low temperatures, and that bombardments near 4.2°K are required to study defects in something like their original configuration. They also show that defects introduced at 4.2°K are modified by subsequent irradiation; vacancy-interstitial pairs are thought to recombine and to be converted to other types of defects by further irradiation.[1] These secondary irradiation effects are related to the excitation of the electronic system and increase in importance as the total flux increases. We shall see that they may be greatly reduced by increasing the sensitivity of measurements of defect concentration and thus reducing the magnitude of the flux needed for low-temperature studies.

A hundredfold increase in sensitivity at 4.2°K is obtained by monitoring the damage introduced into nondegenerate samples with high-field conductivity measurements. Short, infrequent pulses are used to excite electrons by impact ionization from the shallow chemical-donor levels to the conduction band. The use of short pulses limits the lattice heating to a few degrees. Conductivity measurements, made while the electrons are in the conduction band, provide a measure of the number of occupied chemical-donor states. Radiation introduces deeper-lying electron acceptor levels that deplete the electron population of the chemical donors, thus reducing the high-field conductivity. The change in pulse conductivity after irradiation gives an accurate measure of the number of radiation defects.

In addition to increasing the sensitivity of measurements of the defect concentration, pulse measurements have the further advantage that the average carrier energy may be varied over a wide range by varying the pulse voltage. Using this feature, the change in conductivity following irradiation can be separated into contributions from the change in carrier concentration and from the increased charged-impurity scattering. For some defects, it is also possible to measure the cross sections for capturing a conduction-band electron as a function of the carrier energy.

[1] J. W. MacKay and E. E. Klontz, in *Proceedings of the 7th International Conference on the Physics of Semiconductors: Radiation Damage in Semiconductors* (Dunod Cie., Paris, 1965), Vol. 3. The model discussed in this paper pictures a vacancy-interstitial pair as a vacancy and interstitial bound within a few lattice positions of each other and which, given sufficient energy to surmount an intervening potential barrier, can recombine in one or a few jumps.

II. EXPERIMENTAL PROCEDURE

The experiments were performed on Sb-doped germanium with an exhaustion range carrier concentration of about 10^{14} cm^{-3}. Carrier concentrations and resistivities obtained by dc Hall effect and conductivity measurements at 78°K are given in Table I. The samples were ground as rectangular parallelopipeds with approximate dimensions of $1.0\times0.2\times0.015$ cm and then etched in CP_4. Broad end contacts were prepared by soldering platinum plates to the ends of the sample with Sb-doped 50/50 solder and heating the assembly to 400°C for fifteen minutes. This procedure provides good noninjecting contacts to fields of at least 200 V/cm. Small dots of the doped solder were placed on the sample edges before heating and voltage probes were later attached at these points.

Voltage pulses were obtained by discharging a length of RG8U coaxial cable through a mercury-wetted contact relay into a matched load. The pulses were 0.66 μsec long and could be varied in amplitude from 0 to about 300 V by varying the charge on the cable. A simple trigger circuit pulsed the relay at the rate of 0 to 10 pulses/sec (pps). Sample dimensions were selected so that the sample resistance after breakdown was $\geq 200\ \Omega$. The sample and a 100-Ω standard resistor were mounted in series. This combination was shunted by a 55-Ω resistor to provide a load that varied only $\pm 5\ \Omega$ from the characteristic impedance of the cable (50 Ω) during all pulses measurements.

The conductivity was usually determined by four voltage measurements made on the sharply defined trailing edge of the pulse, each measurement being made to ground. The difference between voltages on either side of the standard resistor yields the sample current and the difference between voltages measured at two probes gives the IR drop. On the first two samples in Table I, the voltage drop was taken across the whole sample. Measurements made at probes are preferred because of the difficulty of obtaining uniform irradiation over the entire length of the sample.

TABLE I. Dc electrical parameters of germanium samples.

Sample	Resistivity ρ (Ω cm)	Hall coefficient R (cm^3/C)	Electron concentration $n_H = 1/cR$ (cm^{-3})
Ge(Sb)-268A-10C[a]	0.7676	17430	3.2×10^{14}
Ge(Sb)-309A-2C[a]	1.853	43160	1.4×10^{14}
Ge(Sb)-309A-4C	1.995	52120	1.2×10^{14}
Ge(Sb)-309A-6C	1.776	41260	1.6×10^{14}
Ge(Sb)-309A-7C	1.868	50480	1.2×10^{14}

[a] Pulse measurements made across whole sample.

Pulse voltages were measured with a type-545 Tektronix oscilloscope and a type-Z preamplifier. A distributed amplifier in this oscilloscope delays the measured signal so that it may also be used as the sweep trigger without obscuring the leading edge of the pulse. The preamplifier has a sensitivity of 50 mV/cm and a voltage comparator that allows signals up to 100 V to be measured with this sensitivity. The voltages to be measured ranged from about 10 to 300 V. A fixed, 10$\times$ attenuator was placed in the input to the preamplifier to increase the input impedance. Relative voltage measurements are accurate and reproducible to at least 0.5%. The absolute accuracy of the measuring system is no better than 2 or 3%, but this is of little importance, since the significance of the experimental data depends on the relative measurement of the electrical properties of a single sample.

Three electron accelerators were used for various parts of this work: a Van de Graaff machine with a 0- to 1-MeV dc beam; a pulsed, traveling-wave linear accelerator with energy variable from 0.4 to 1.5 MeV; and a 2.5- to 5-MeV pulsed linear accelerator. On all three machines, an analyzing magnet confines the energy spread of the electron beam to about 3%. The analyzer calibrations are accurate to $\pm 1\%$. The bombardment rates used were $\lesssim 6\times 10^{11}$ electrons/cm^2 sec (0.1 μA/cm^2). The total irradiation flux was measured by discharging collected charge through calibrated ballistic galvanometers. Because of the small total fluxes used, switching voltages and charge leakage limited the accuracy of the flux measurements to $\pm 10\%$.

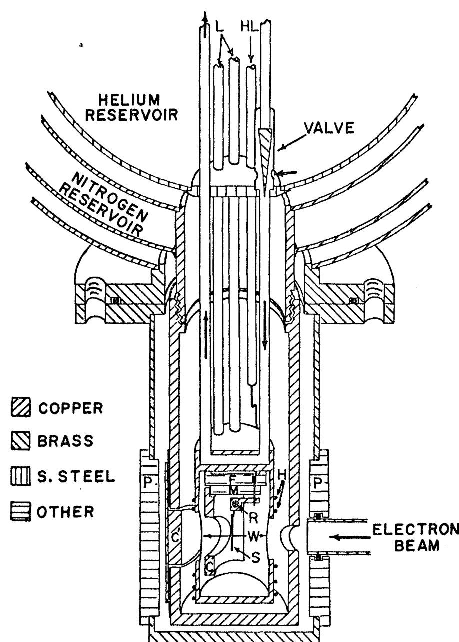

FIG. 1. Tailpiece of liquid-helium cryostat. Heavy arrows show direction of helium flow. Other symbols identified in text.

Bombardments were made in a metal cryostat whose general description is given elsewhere.[2] A view of the tailpiece is shown in Fig. 1. Eight thin-walled stainless-steel tubes descend from the spherical liquid-helium reservoir. Two form a U tube that carries liquid helium to the sample chamber when the valve is open; five (L) carry separately shielded leads and helium exchange gas into the sample chamber, and one (HL) provides a lead to the heater (H) wound on the outside of the sample chamber. The sample (S) is mounted on an 8-pin plug (M) which is mated with a receptacle (F) permanently wired in the chamber. Six of the plug pins are used for sample leads, and two provide connections to the carbon composition resistor (R) used as a thermometer between 4 and 78°K. Beam collectors C and C′ stop scattered and unscattered electrons, respectively. Directly opposite C′, a hole in the thermal shield attached to the liquid-nitrogen reservoir, collimates and defines the incident electron beam. In order to isolate the chamber from the vacuum 0.001-in. Al windows (W) are used.

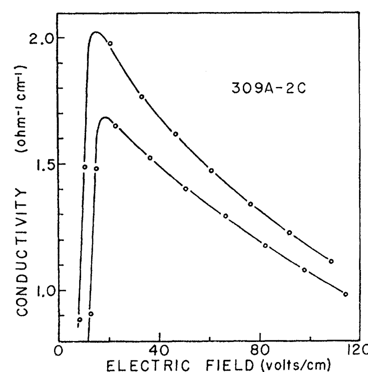

FIG. 2. Conductivity as a function of pulse field. Upper curve taken before, and lower curve after irradiation by 1.0-MeV electrons.

A nontransparent window is used because the electrical properties of some of the defects studied are very sensitive to thermal radiation. In annealing experiments, the valve in the helium container is closed and current is supplied to the heater.

The tailpiece of the cryostat is set between the poles (P) of a magnet which provides fields to 2500 G for Hall-effect measurements. The bombardment beam passes through a $\frac{1}{2}$-in. hole in one magnet pole, thus allowing both the beam direction and the magnetic field to be perpendicular to the broad face of the sample.

III. HOT-CARRIER EFFECTS

When a voltage pulse is applied to the specimen, energy is supplied to the electrons. Initially they gain energy more rapidly than they can pass it on to the lattice and the average energy of the electron system

[2] J. E. Whitehouse, T. A. Callcott, J. A. Naber, and J. S. Raby, Rev. Sci. Instr. 36, 768 (1965).

increases. The frequency of electron-lattice collisions increases with average carrier energy until finally the electron system loses energy at the same rate that it is supplied by the electric field. This steady state is achieved in a time short compared to the voltage pulse duration, so that the conductivity measured during the pulse is characteristic of a carrier temperature much higher than the lattice temperature.[3] Of course the lattice temperature rises too, but, since the specific heat of the lattice is much larger than the specific heat of the electrons, its temperature increase is much smaller.

The pulse conductivity, measured during pulses of specified amplitude, is shown as a function of pulse field in Fig. 2 for a typical sample. The upper curve was taken before, and the lower curve after irradiation by 1.0-MeV electrons. The shape of either of the curves may be qualitatively explained as follows. At the lowest pulse-field values, the steady-state electron temperature achieved during the pulse is not high enough to produce full ionization of the donors. As the field increases, ionization and conductivity increase.[4] Complete ionization is probably achieved somewhere below the conductivity maximum in Fig. 2, but the conductivity continues to rise with field because the mobility, which at low electron energies is dominated by charged-impurity scattering, increases with increasing electron temperature. Above the conductivity maximum, lattice scattering becomes dominant and the mobility and conductivity decrease with increasing carrier temperature. A detailed theoretical explanation of the curve is extremely complex.[5] It must take into account many scattering mechanisms. In addition, the form of the distribution function is determined by the dependence of the relaxation times of the various scattering mechanisms on the carrier energy. In general, the carriers in the band will not have a Maxwellian velocity distribution.

For our purposes, no attempt need be made to analyze the hot-carrier mobility in detail. A calculation of the carrier temperature as a function of the pulse field is discussed in the Appendix. This calculation requires direct consideration only of inelastic-scattering processes that result in significant energy losses. Elastic processes that change only momentum can be ignored. The result of the calculation is given in Fig. 3 for assumptions yielding minimum and maximum carrier temperature for a given pulse field.

[3] A carrier temperature T_e completely defines the carrier system if the carriers have a Maxwellian velocity distribution. For non-Maxwellian distributions, the concept of carrier temperature may be retained as a convenient measure of the average carrier energy when defined by the expression $\langle E\rangle=\frac{3}{2}kT_e$, where $\langle E\rangle$ is the carrier energy averaged over the appropriate distribution function.

[4] S. H. Koenig and G. R. Gunther Mohr, J. Phys. Chem. Solids 2, 268 (1957); also N. Sclar and E. Burstein, *ibid.* 2, 1 (1957).

[5] E. G. S. Paige, *Progress in Semiconductors* (Heywood and Company Ltd., London, 1964), Vol. 8, pp. 178–213. This book-length monograph on conductivity of germanium may be consulted for references to, and comments on, the numerous papers devoted to the measurements and calculations of hot-carrier mobilities.

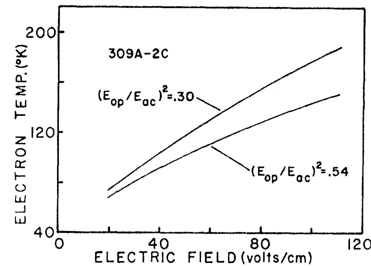

FIG. 3. Calculated electron temperature versus pulse field for two ratios of optical- to acoustic-mode lattice scattering.

The maximum possible temperature rise of the sample during a high-voltage pulse may be simply calculated, assuming adiabatic heating and a specific heat that varies as $C(T_L)=C_0(T_L/T_0)^3$, where C_0 is the specific heat at a temperature T_0, and T_L is the lattice temperature after a pulse of length Δt. The result is

$$T_L=T_0\left(\frac{4\sigma E^2\Delta t}{C_0T_0}+1\right)^{1/4}. \tag{2}$$

In germanium at 4.2°K, $C_0\simeq 2\times10^{-4}$ J/cm^{-3}°K.[6] The maximum temperature rise calculated for the samples discussed in this paper is about 5°K, for fields of 100 V/cm, and 7°K for fields of 200 V/cm.

IV. RADIATION-INDUCED CHANGES IN CONDUCTIVITY

The lower curve in Fig. 2 is the pulse conductivity measured after irradiation has introduced defect-acceptor levels below the Sb chemical levels. At a given carrier temperature, for fields above the conductivity maximum, and for reasonably small changes in the conductivity, the change in conductivity due to irradiation may be written

$$\frac{\Delta\sigma}{\sigma_0}=\frac{\Delta n}{n_0}+\frac{\Delta\mu}{\mu_0}, \tag{3}$$

where σ_0 and μ_0 are the conductivity and mobility before irradiation at a given carrier temperature, and n_0 is the exhaustion-range carrier concentration. Δn is the change in carrier concentration due to irradiation and is given in the pulse, as in the dc case, by Eq. (1). $\Delta\mu$ is the decrease in mobility caused by the introduction of charged scattering centers. Since charged impurity scattering does not contribute significantly to the energy losses of the carrier system, the energy loss per carrier is the same before and after irradiation. Therefore equal carrier temperatures are obtained for equal

[6] P. Flubacher, A. J. Leadbetter, and J. A. Morrison, Phil. Mag. 4, 273 (1959).

average power input per carrier, i.e., when

$$E_0^2\frac{\sigma_0}{n_0}=E^2\frac{\sigma_0+\Delta\sigma}{n_0+\Delta n}, \qquad (4)$$

where E_0 and E are the fields before and after the introduction of defects.

At high electron temperatures, where impurity scattering is negligible in comparison to lattice scattering, the mobility is not significantly changed by irradiation and (3) and (4) reduces to $\Delta\sigma/\sigma_0\simeq\Delta n/n_0$ and $E_0\simeq E$. Thus, at sufficiently high fields, the carrier-temperature isotherms become vertical lines on a conductivity–versus–electric-field plot, and the change in conductivity at a given field is proportional to the change in carrier concentration. Figure 4 shows the percent change in conductivity produced by irradiation as a function of electric field, taken from the conductivity curves of Fig. 2. The change in conductivity attributable to charged-impurity scattering is small above about 80 V/cm, so that above this field it is reasonably accurate to set $\Delta\sigma/\sigma_0=\Delta n/n_0$ and $E_0=E$.

V. EXPERIMENTAL RESULTS

The pulse conductivity observed immediately after irradiation is smaller than the prebombardment value. However, the value of the conductivity measured at a given field is not stable but continues to decrease under repeated pulsing. With continued pulsing the conductivity finally approaches a limiting value. If a short burst of ionizing irradiation (x rays or electrons) is applied to the sample, the conductivity is returned to the value found immediately after bombardment. Further application of the pulsed field, or brief warming of the specimen to 15°K, will then return the conductivity to the same limiting value as before. This behavior indicates that the specimen does not have an equilibrium electron distribution between the radiation defects and chemical impurities immediately after irradiation.

The trapping properties of the specimen may be understood with the aid of Fig. 5. In Fig. 5(a), band-to-band ionization, accompanying x rays or energetic electrons, produces electron-hole pairs; the holes are trapped with high probability on the defect state, and the electrons with high probability on the chemical-donor levels, thus effectively transferring electrons from the defect levels to the chemical-doping levels. When the source of ionization is removed, the defects are left with less than their equilibrium quota of electrons. So long as the carriers are frozen out on the chemical donors, equilibrium cannot be restored. Processes that preferentially ionize the Sb levels, such as heating the sample or applying voltage pulses to it, allow the radiation defects to capture their quota of electrons from the conduction band. The filling process is shown schematically in Fig. 5(b). This explanation requires that the defect has a large capture cross section for holes and a small capture cross section for electrons, as is shown to be the case in a later section of this paper. For the present, it is enough to note that to obtain an accurate and reproducible measure of the conductivity change induced by irradiation, it is necessary to heat the sample to about 15°K for a short time.

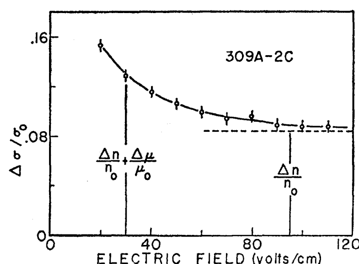

FIG. 4. Radiation-induced conductivity changes. At higher fields, the change is largely attributable to change of carrier concentration ($\Delta n/n_0$).

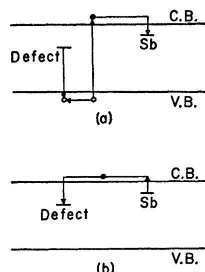

FIG. 5. Electronic transitions determining defect population. (a) Defect emptying by band-to-band ionization. (b) Defect filling by preferential ionization of Sb donors.

A. Isochronal Annealing

Isochronal annealing was performed on sample Ge(Sb)-268A-10C after irradiation with 1-MeV electrons produced a total change in conductivity of about 20%. The sample was quickly heated to the annealing temperature and held there for 7 min. It was then rapidly cooled to 4.2°K and a conductivity-versus-field curve was taken. In Fig. 6, curve A shows the percent of radiation induced conductivity change that has been recovered in all anneals up to the plotted temperature. The conductivity measurements were made at a pulsed field of 70 V/cm. Curves B and C of Fig. 6 show, for comparison, similar isochronal annealing results taken by dc measurements on degenerate samples.[7,8] Note that the total fluxes used on the degenerate sample are about 20 and 100 times greater than used on the purer sample.

It is evident from Fig. 6 that the annealing in the purer specimen is remarkably similar to that in the degenerate specimen except that the percentage of recovery is much higher. It is reasonable to conclude

[7] E. E. Klontz and J. W. MacKay, J. Phys. Soc. Japan 18, Suppl. III, 1216 (1963).
[8] J. W. MacKay and E. E. Klontz, *Radiation Damage in Solids* (International Atomic Energy Agency, Vienna, 1963), Vol. III, p. 27.

that the annealing process is the same for heavily doped and lightly doped germanium and is independent of impurity concentration. The annealing kinetics must have a first-order dependence on defect concentration since there is no dependence of the annealing temperature on the number of defects. These observations are consistent with the interpretation of the 65°K annealing stage as a recombination of correlated close vacancy-interstitial pairs. The much larger percent recovery in the pure specimen is evidently a continuation of the trend that can be seen by comparing curves B and C in Fig. 6. The percent recovery decreases as the irradiation flux increases. This behavior is interpreted as indicating radiation annealing and conversion of the close pair defects that are responsible for the 65°K annealing stage. We will further discuss these secondary radiation effects in Sec. V D.

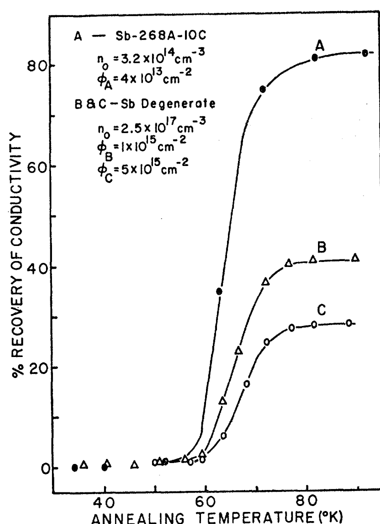

FIG. 6. Isochronal annealing of n-type germanium at 65°K. n_0 is the prebombardment exhaustion-range carrier concentration and φ is the flux of 1.1-MeV electrons. Data on the degenerate sample taken by E. Klontz.

B. Electron-Capture Times for Radiation Defects

As we have noted, following irradiation the 65°K defects (as we will hereafter identify the defects annealing at 65°K) are left in a nonequilibrium empty state, and may be filled by applying a pulse field that preferentially ionizes the chemical donors and allows the defects to capture their quota of electrons. We have made use of this effect to measure the electron trapping cross section of the defect as a function of carrier energy. After emptying the defects with x rays, the refilling time was measured at several pulse fields. The decrease in conductivity accompanying the capture of electrons on the defect was monitored in each case at 36 V/cm, where measurements could be made in a time short compared to the characteristic filling time at that field. The time the carrier distribution remains at a

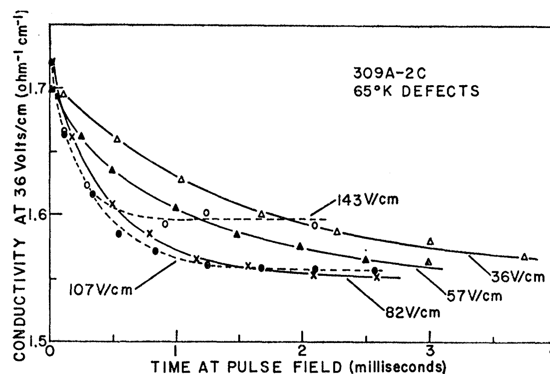

FIG. 7. Conductivity changes during filling of 65°K defect by voltage pulses.

temperature corresponding to one of the applied fields was measured by counting the number of pulses and multiplying by the pulse length.

The results of measurements made on a sample irradiated by 1.0-MeV electrons are shown in Fig. 7. At this bombardment energy, approximately 80% of the total conductivity change is due to defects that anneal at 65°K. The curves for the 36-, 57-, and 82-V/cm applied fields all approach the same final value of the conductivity as observed at 36 V/cm, after heating the sample to about 20°K. The crossover of the 107- and 143-V/cm curves indicate that at these fields, defects as well as Sb impurities are being ionized to some extent. The curves were analyzed as exponentials. The characteristic time for capturing a conduction electron, as measured by the characteristic times for the conductivity to decay toward a final value, are plotted as a function of pulse field and calculated electron temperatures in Fig. 8. The electron temperatures are taken from the lower curve of Fig. 3, which was calculated for this sample. The dashed curves in Fig. 8 are obtained by multiplying the number of pulses by the full 0.66-μsec pulse length. The solid line is obtained by multiplying by the portion of the pulse that follows the spike on the leading edge of the pulse that identifies the

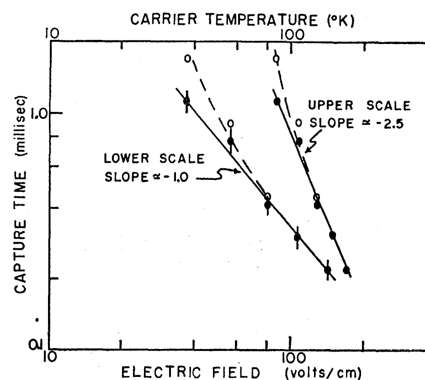

FIG. 8. Characteristic filling times of 65°K defect as a function of electric field and calculated electron temperature.

avalanche breakdown of the Sb impurity levels. At 36 V/cm, this spike extends over about a third of the pulse length, while at fields $\gtrsim 100$ V/cm the avalanche is complete in less than the rise time of the pulse. The dashed and solid curves serve to indicate minimum and maximum estimates of the characteristic capture time at each field.

The capture cross section of a defect for conduction-band electrons may be written

$$\alpha = 1/nv\tau, \quad (5)$$

where n is the number of conduction-band electrons available for capture, v is the electron velocity, proportional to $T_e^{1/2}$, and τ is the characteristic capture time. From Fig. 3 a field of 40 V/cm corresponds to an electron temperature of about 100°K. Using this temperature and $n \simeq 1.4\times 10^{14}$ cm^{-3} the capture cross section at this field is $\alpha \cong 10^{-18}$ cm^2. Figure 8 indicates a temperature dependence of $\alpha \propto T_e^2$ (approximately). Both the magnitude of the capture cross section and its dependence on carrier energy indicate that the defect is a negative defect capturing a second electron.[9] The added electron energy aids in penetrating the Coulomb barrier to electron capture.[10] This temperature dependence is usually, but not always, seen for electron capture cross sections on negative centers; positive and neutral centers have larger capture cross sections with the opposite temperature dependence, if any.[11]

We thus conclude that the defect that anneals at 65°K has a double negative charge in its equilibrium state. As further evidence for this view, we may note that the conductivity change observed after irradiation at a given field ($E > 80$ V/cm) with the defects full (doubly charged) is about twice that observed with the defects empty (singly charged).

After annealing to 90°K, samples were heated and dosed with x rays to determine if any of the remaining defects showed nonequilibrium conductivity effects. For irradiations between about 0.7 and 4.5 MeV, no such effects were observed. After irradiations at 0.5 and 0.6 MeV, where much larger fluxes are required to produce measurable damage, nonequilibrium effects were still present after annealing. Thus high fluxes (rather than high energy) produce defects with nonequilibrium behavior that remain after annealing to 90°K. The above experiment of emptying defects by

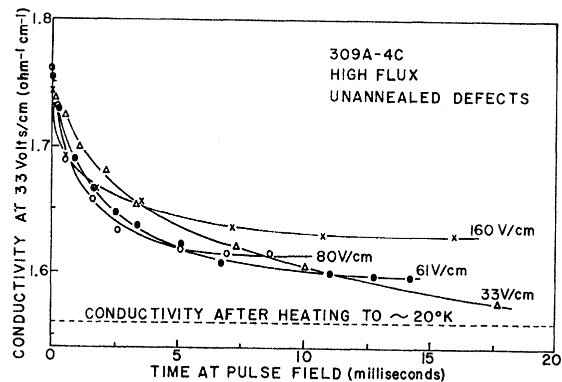

FIG. 9. Conductivity changes during filling of unannealed defects produced by large fluxes at 0.5 MeV.

x rays and refilling them at various pulse fields was therefore repeated for a sample irradiated at 0.5 MeV and annealed to 90°K. The results are shown in Fig. 9. The conductivity decay curves are similar to those observed for the 65°K defects (Fig. 7) except that the curves obtained after pulsing at each field approach a different final value of the conductivity. Only the curve obtained after pulsing at 33 V/cm, the field at which the conductivity changes were monitored, approaches the final conductivity value obtained at that field after heating the sample. Pulsing at higher fields results in a higher final conductivity. This implies that electrons are excited from the defects to the conduction band by the applied field, at least at field values above 33 V/cm, and that the final conductivity is determined by the relative excitation and recombination rates of the Sb impurities and radiation defects. Without a detailed analysis of the decay curves, we may conclude that these defects, like the annealable defects, have a double negative charge in their equilibrium state, but that their second electron is more easily ionized at low pulse fields.

Since the relative electron populations of these damage centers and the Sb impurities change as the pulse field changes, conductivity–versus–pulse-field curves are not easily reproducible and cannot be readily interpreted. This fact serves to limit useful measurements of removal rates to bombardment energies where these defects do not dominate the changes in the conductivity; in our case to energies ≥ 0.6 MeV.

In later paragraphs, we argue that this defect is produced by radiation conversion of the 65°K defect. This conclusion draws support from the similar electron-capture behavior of the two defects. Modification of the 65°K defect by separation ot its vacancy interstitial components has been previously proposed to account for the data of Kortright[12] and Klontz.[7,8] Such separation could result in a stable defect with similar properties if it results in a more widely spaced pair or in a

[9] B. K. Ridley and T. B. Watkins, Phys. Chem. Solids 22, 155 (1961).

[10] B. K. Ridley and R. G. Pratt, J. Phys. Chem. Solids 26, 11 (1965); also V. L. Bouch-Bruevich, Fiz. Tver. Tela 1, 186 (1959) [English transl.: Soviet Phys.—Solid State 1, 166 (1959)]. These papers indicate that tunneling through the Coulomb barrier is the dominant process controlling the temperature dependence of the capture cross section.

[11] A fair sampling of capture cross sections is given in the following: (a) V. G. Alexeeva *et al.*, Phys. Chem. Solids 22, 45 (1961); (b) R. L. Williams, *ibid.* 22, 267 (1961); (c) E. M. Conwell and J. Zucker, *ibid.* 22, 141 (1961); (d) G. Rupprecht, *ibid.* 22, 255 (1961). See also L. Johnson and H. Levinstein, Phys. Rev. **117**, 1191 (1960).

[12] J. M. Kortright, Ph.D. thesis, Purdue University, 1963 (unpublished).

complex of the vacancy with a chemical-impurity center.

C. Bombardment Energy Dependence of Damage and Annealing Effects

The essentials of the annealing experiment described above were repeated at bombardment energies in the range 0.6 to 4.5 MeV. At each energy, the removal rate was measured. The sample was then annealed at 50 and 90°K to determine the percent recovery in the 65°K annealing range. No changes were observed at 50°K. Data taken from the changes in conductivity measured at 120 V/cm are shown in Figs. 10 and 11. The percent recovery of the conductivity in the 65°K annealing range is shown as a function of the bombardment energy in the upper curve of Fig. 10. The lower curve of that figure is the percent recovery observed in degenerate material. Since the percent recovery at a given bombardment energy is a measure of the conductivity change at that field attributable to the annealable defects, the data indicate that about 95% of the conductivity change is due to these defects after 0.7-MeV irradiation of the pure sample. The decrease in the percent recovery toward higher bombardment energies is interpreted as due to increased production of defects requiring larger displacement energies than the 65°K defect. The decrease below 0.7 MeV, on the other hand, is attributed to radiation modification of the 65°K defect by the heavier fluxes necessary to produce measurable damage at low energies. The lower recovery observed at all energies for the degenerate sample is also believed to be due to radiation modification of previously introduced defects. These points are discussed further in Sec. V D on secondary radiation effects.

Figure 11 shows three removal rates observed at 4.2°K as a function of bombardment energy: the removal rate associated with all electrically active defects, that associated with the 65°K defect only, and that associated with defects remaining after annealing. The curve for the 65°K defects is obtained by multiplying the percent recovery curve of Fig. 10 by the total-removal-rate curve. This result subtracted from

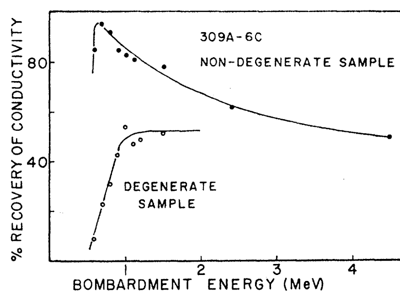

FIG. 10. Bombardment-energy dependence of the recovery of conductivity in the 65°K annealing stage. Data on degenerate sample taken by E. Klontz.

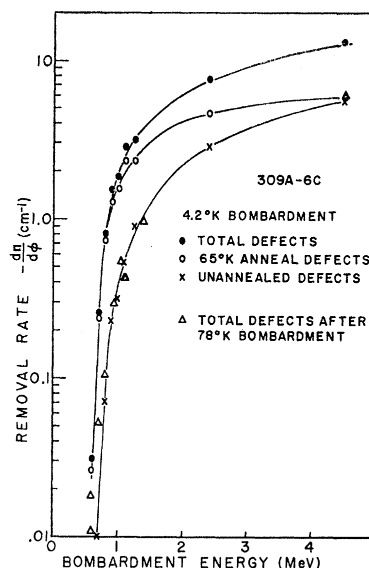

FIG. 11. Bombardment-energy dependence of experimental removal rates. 78°K data taken by J. Kortright.

the total curve yields the conductivity changes associated with the unannealed defects.

In Fig. 11, the removal rate observed by Kortright in n-type germanium at 78°K using low flux rates ($<10^{12}$ cm^{-2} sec^{-1}) of energetic electrons are plotted as solid triangles.[12] They fall almost directly on top of the curve representing the defects that are left after annealing similar material irradiated at 4.2°K. We suggest that the defects responsible for the conductivity change in each case are identical. The qualification of low flux rates is important for the 78°K data, since Kortright observed the defect introduction rate to be strongly dependent on the beam current, particularly for energies below 1 MeV. The flux-rate-dependent portion of the removal rate is interpreted by Kortright and MacKay to be due to conversion of 65°K defects to permanent defects before they can annihilate. We suggest here that the residual removal rate at 78°K is due to the production of primary defects requiring greater displacement energy than the annealable defects.

In Fig. 12, the total observed removal rate, indicated by solid points, is compared to simple displacement theory which assumes a step function displacement energy E_d for directly produced defects, and that recoiling atoms where energy $>E_d$ may produce secondary displacements.[13] A reasonably good fit is obtained to the theory for a displacement energy of 27.5 eV, assuming two electrons removed per defect. The latter number is scarcely significant because of the crudity of several assumptions of the theory. The absolute threshold for producing damage in n-type

[13] F. Seitz and J. S. Koehler, in *Solid State Physics*, edited by F. Seitz and D. Turnbull. (Academic Press Inc., New York, 1956), Vol. 2, pp. 328–333, 380–388.

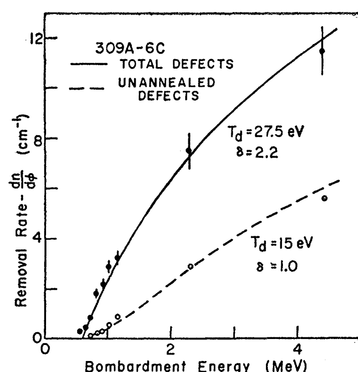

FIG. 12. Comparison of experimental removal rates to displacement theory. T_d is the assumed threshold energy, and δ the electrons removed per defect. The solid line indicates single defects, and dashed line defects requiring two or more displacements for their formation.

germanium is known to be at least as low as 15 eV.[14] Consequently, this threshold value, applicable to bombardment energies transferring energy well above the "true" threshold, must be interpreted as some mean between the minimum possible displacement energy and the energy at which the probability of stable defect production approaches 1.[15] Near the threshold, where large fluxes are required to produce measurable damage, radiation annealing effects will also contribute to a reduction in the removal rates, thus increasing the apparent energy of the threshold.

The open circles in Fig. 12 are the observed removal rates of the defects remaining after the anneal to 90°K. At energies above 0.6 MeV, these are thought to be directly produced and not converted defects. The dotted curve represents the number of secondary displacements calculated by subtracting the number of primary displacements from the total number of displacements. Defects resulting from secondary displacements may be distinguished from primary defects only if they are a different type of defect; most plausibly if they are double vacancies or divacancies. The latter term refers to adjacent vacancies, and the former to separated, but associated, vacancies. This experimental result suggests that the unannealed defects produced by high energies (as contrasted to those associated with high fluxes at energies $\lesssim$0.6 MeV) represent multiple defects; and the fact that they are electron acceptors suggests that they are multiple vacancies, perhaps with associated interstitials. Two other observations may be mentioned that lend some support to this interpretation. The prevalence of close-spaced vacancy-interstitial pairs for energies above the damage threshold suggests that most displaced atoms quickly lose their energy to surrounding atoms, and thus that closely spaced double vacancies should be produced with high probability. Also, it is known that di-vacancies form a very stable defect structure in silicon,[16] which has the same lattice structure as germanium. An alternative explanation for the shape of the curve associated with the nonannealed defects requires the assumption of a threshold function for the production of defects that rises from zero to one over a very wide range of displacement energies.[17]

If our suggestion that the unannealed defects are primarily multiple defects is substantially correct, the 15-eV threshold value for each displacement that was used to obtain a fit to the data represents a transferred energy at which displacements occur with very nearly unit probability. The higher threshold value observed for the production of stable single defects must then be accounted for by assuming that all single displacements do not form stable defects and/or that radiation annealing effects falsify the observed threshold.

The conclusion that the unannealed defects are double vacancies is consistent with the theoretical fit obtained for the total number of defects in Fig. 12 only if the double vacancies carry a greater total charge than the 65°K defects. Otherwise secondary displacements which yield associated vacancies would not add to the electron-removal rate as that requires. It is our belief that calculations of the total number of defects, based on a simplified model giving only the number of energetically possible displacements, is not reliable enough to justify such a conclusion about the charge state of the unannealed defects. The rather unusual S shape of the curve for the unannealed defects seems to us to have greater significance.

Assuming that bombardment produces either single 65°K defects or double vacancies, the calculation of the number of single defects requires that the number of secondaries producing double vacancies be subtracted from the total number of primary displacements, i.e., it requires the subtraction of the two curves we have fitted in Fig. 12. The result is not included since it gives no new information.

D. Secondary Radiation Effects

To launch a discussion of radiation annealing and conversion, consider their effects on the type of data shown in Figs. 10 and 11. Assume that defects anneal-able at 65°K are modified by irradiation and that other defects are not, and that 96% of the defects formed are of the modifiable type. These conditions should be approximately valid for bombardments of 0.7 MeV and below. Figure 10 gives a measure of the ratio of 65°K to total defects observed after a given irradiation, and would give that ratio directly if all the defects had the same charge state. If, for example, one-half of the 65°K defects introduced were *radiation annealed* (i.e.,

[14] J. J. Loferski and P. Rappaport, J. Appl. Phys. **30**, 1296 (1959); Phys. Rev. **111**, 432 (1958).
[15] J. W. Corbett *et al.*, Phys. Rev. **108**, 954 (1957).
[16] J. W. Corbett and G. D. Watkins, Phys. Rev. Letters **7**, 314 (1961); Phys. Rev. **138**, A545 (1965); **138**, 555 (1965).
[17] W. L. Brown and W. M. Augustyniak, J. Appl. Phys. **30**, 1300 (1959).

annihilated) during subsequent bombardment, we would still observe that 92% of the total defects were thermally annealed at 65°K. If, however, one-half of the defects were *radiation converted* to unannealable types, we would observe only 48% of the total number of defects to be annealable at 65°K. Clearly, radiation conversion has by far the greater effect on the data as plotted in Fig. 10. Figure 11 gives a measure of various defect production rates as a function of bombardment energy. Radiation annealing would sharply reduce the total observed removal rate, while radiation conversion would have no effect so long as charge states before and after the conversion were the same. Both secondary irradiation effects would, of course, reduce the absolute numbers of 65°K defects observed after heavy irradiations. Thus either effect could give rise to a spurious threshold for the production of 65°K defects, but only radiation annealing should seriously affect the total-removal-rate threshold.

The percent recovery in the 65°K annealing range plotted in Fig. 10 is very sensitive to radiation conversion. The decrease in percent recovery below 0.7 MeV in the pure sample, and the lower percent recovery observed at all energies in the degenerate sample, is attributed to this effect. This interpretation is consistent with our previous result that a second type of unannealed defect showing nonequilibrium conductivity effects is present in pure material, after heavy irradiations at 0.5 and 0.6 MeV, but is not observed at higher energies where much smaller total fluxes are used. It also agrees with measurements[7] on degenerate material that identify defects whose production depends on a previous population of 65°K defects being present in the sample, and thus are thought to be produced by radiation conversion. In Fig. 10 then, as well as in Fig. 6, the higher percent recovery during annealing in the pure sample is a consequence of the reduction in radiation conversion that accompanies the reduction in total flux required to produce measurable damage.

That radiation annealing also occurs in the nondegenerate material was demonstrated directly by the following experiment: Sample 309A-7C was irradiated with 1.0-MeV electrons until a 20% change in conductivity had occurred. Further irradiation at 0.5 MeV

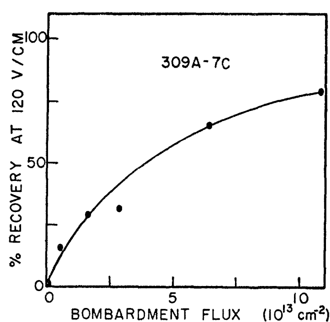

FIG. 13. Radiation annealing in nondegenerate n-type germanium.

TABLE II. Total fluxes used in bombardments of sample 309A-6C.

Bombardment energy (MeV)	Flux (10^{13} cm^{-2})
4.5	0.25
2.5	0.40
1.5	Unknown
1.25	0.56
1.1	0.69
1.0	1.31
0.9	1.42
0.8	2.58
0.7	8.06
0.6	58.4

introduced negligible numbers of additional defects but caused the recovery in conductivity shown in Fig. 13. Results of a similar experiment on degenerate material show a smaller recovery of about 40% after 100 times larger fluxes.[18] For both types of material, subsequent thermal annealing to 90°K gives only a few percent additional recovery of the conductivity. In the pure sample, there is no evidence of converted defects until much larger fluxes are used, and in the degenerate sample, at least a portion of the conductivity recovery is associated with radiation annealing. Though the total fluxes used on the nondegenerate samples discussed here are about two orders of magnitude smaller than for the degenerate samples, Fig. 13 indicates that radiation annealing effects are 100 times larger per unit flux, giving no net decrease in radiation annealing from using smaller fluxes on lightly doped samples. This surprising result strongly reinforces our previous conclusion that the difference in percent recovery observed in pure and degenerate n-type germanium is related primarily to a difference in the total radiation conversion in the two types of samples, radiation conversion being larger when larger fluxes are used.

It is clear that radiation annealing will strongly affect the removal rate observed at 0.5 MeV if total fluxes larger than about 2×10^{13} cm^{-2} are used. Such a 0.5-MeV irradiation was attempted, but very few defects were found after fluxes of more than 10^{16} eV/cm^2. Instability in the pulse conductivity indicated the presence of converted defects, but made the reliable measurement of a small population of 65°K defects impossible. Since ionization per unit path length of a bombarding electron, upon which radiation annealing depends, decreases in the energy range from 0.5 to 1.0 MeV and becomes nearly constant from 1.0 to 5.0 MeV,[19] the radiation annealing per unit flux observed at 0.5 MeV represents a maximum value for all higher energies of interest to us. Table II gives the total fluxes used at each energy in obtaining the energy-dependent damage and annealing effects plotted in Figs. 10 and 11. If radiation annealing effects per unit flux remain

[18] J. W. MacKay and E. E. Klontz, J. Appl. Phys. **30**, 1269 (1959).

[19] F. Seitz and J. S. Koehler, in *Solid State Physics*, edited by F. Seitz and D. Turnbull (Academic Press Inc., New York, 1956), Vol. 2, pp. 347–350.

approximately constant for bombardments at and above 0.5 MeV, from this table and Fig. 13 we can conclude that radiation annealing will be important at fluxes above about 2×10^{13} cm^{-2} and hence for bombardment energies $\leq$0.8 MeV. Adjusting the experimental removal rates for such annealing before comparing them to the theoretical model in Fig. 12 would reduce the effective threshold obtained for total damage from 27.5 MeV to about 22 eV. Such strong radiation annealing should also cause curvature in a plot of the number of defects produced as a function of radiation flux, since increasing numbers of defects would be annealed as the population of defects builds up, while the defect production rate would remain constant. In particular, for the large fluxes used at 0.6 MeV, the number of defects should have approached an equilibrium value at which defects are being annihilated as fast as they are produced. No such saturation effect is observed at 0.6 MeV, nor is there significant curvature in the plot of defects produced versus flux at 0.7 and 0.8 MeV.

Assuming that the radiation annealing data of Fig. 13 and the removal rates measured in the range of 0.6 to 1.0 MeV are both accurate, the resolution of these results seems to require a large decrease in the radiation annealing per unit flux between 0.5- and 0.6-MeV bombardments. It should be noted, however, that the evidence for very strong annealing at 0.5 MeV and much weaker annealing at 0.6 MeV comes from different types of measurements and unrecognized factors may be influencing the differing results. If further radiation annealing experiments establish such a strong energy dependence, it will have important consequences for the explanation of radiation annealing effects. The energy dissipated per unit path length decreases only slowly in the energy range from 0.5 to 1.0 MeV. Thus the difference in radiation annealing cannot be accounted for by an increased density of ionized electrons or any other process depending approximately linearly on the dissipated energy. A localized heating of the electron distribution, and an exponential dependence of radiation annealing on this local temperature might provide a possible explanation. There is other evidence indicating that local heating is important in the radiation annealing process. It is evident from our measurements on lightly doped material that the defects are stable at the irradiation temperature even without the second electron, since this is the state in which they are found following irradiation. Thus it appears that simply ionizing the defects is not sufficient to produce radiation annealing. Additional energy must be supplied by the incident electrons.

We may summarize the results on secondary irradiation effects as follows: (1) Total radiation-conversion effects are smaller in pure than in degenerate germanium because smaller fluxes are used to produce damage in the pure material. Radiation conversion per unit flux in the two materials are probably comparable. (2)

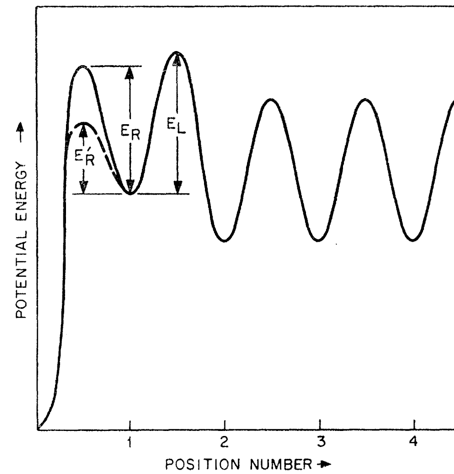

FIG. 14. Potential energy of an interstitial in the neighborhood of a vacancy. Solid and dotted lines give the potential with and without stabilizing electron, respectively.

Present results indicate that at 0.5 MeV, radiation annealing per unit flux is much larger in the pure than in the degenerate material. They also indicate a strong decrease in annealing effects in pure germanium at energies above 0.5 MeV. Further work is planned to check the validity of the latter conclusion.

These results are consistent with a previously described model of the 65°K defect.[8] In this model, the defect is postulated to be a vacancy interstitial pair. In Fig. 14 the potential seen by the interstitial is plotted schematically as a function of available lattice sites at increasing distance from the vacancy. There are potential barriers to both recombination and separation of the pair of energy E_R and E_L, respectively. These two barriers are of nearly equal height when the defect is in its equilibrium charge state. The removal of a stabilizing electron from the defect pair lowers the recombination barrier to E_R', while there is no evidence for a similar effect on the liberation barrier. Radiation annealing occurs when an interstitial is thermally excited by localized heating from the electron beam over the recombination barrier, while radiation conversion occurs by excitation over the separation barrier. Annihilation is favored over liberation when the barrier to recombination is lowered by removing an electron from the defect. In degenerate material, this electron is quickly replaced from the large supply of conduction-band electrons, whereas this source of replacement electrons is absent in pure material at 4.2°K. The greater radiation annealing per unit flux in the pure material is attributable to the increased probability of a defect being found in its ionized state during irradiation. If this interpretation is correct it suggests that the rate of radiation conversion is smaller than the recombination rate with a reduced barrier, but is comparable to the recombination rate when an electron is trapped on the defect.

VI. SUMMARY AND DISCUSSION

We have obtained information on three types of defects produced by radiation in the energy range from 0.5 to 1.0 MeV. The first of these is thought to be the close-spaced vacancy-interstitial pair produced with lowest energy by the electron beam, since it accounts for most of the damage introduced near the threshold, but at energies high enough for secondary irradiation effects to be small. It is doubly charged in its equilibrium state, as demonstrated by the rate at which it traps its second charge from hot electrons in the conduction band. It anneals thermally in times of the order of minutes near 65°K. The dynamics of this anneal indicate that it is controlled by the rate at which an electron is excited from the pair. And finally, it is very sensitive to both radiation annealing and conversion by the ionizing effect of the bombarding electron beam.

A second type of defect is produced by large fluxes at low energies and is believed to be formed by radiation conversion of the above defect. It too traps a conduction band electron at a rate suggesting that it is doubly charged in its equilibrium state. This defect may be associated with a single vacancy in combination with some other component. A third defect has been tentatively identified as a multiple vacancy on the basis of the bombardment-energy dependence of its production rate. This rate of production was shown to be the same as that observed after irradiation at low flux rates at 78°K.

Recently reported results of Whan[20,21] on the formation in germanium of a vacancy-oxygen complex by annealing at 60–70°K, following irradiation at 20°K, have led to speculation[22,23] that the annealing stage at 65°K is not vacancy-interstitial annihilation but long-range migration of the vacancy to form vacancy-impurity complexes of the type that have been reported for silicon. Whan points out,[21] and we would like to emphasize, that while her results do imply that long-range migration occurs for a small fraction ($\sim$0.5%) of the defects formed in heavily irradiated germanium, they do not conflict with the interpretation that the major part of the annealing is vacancy-interstitial annihilation.

Our results indicate: (1) The annealing temperature is independent of doping impurity concentration and, therefore, the formation of centers analogous to the silicon E center cannot be an important part of the annealing stage; (2) the annealing stage is independent of defect concentration and, therefore, long-range migration of the vacancy to form the divacancy cannot be important; nor can the annealing be due to long-range migration of uncorrelated vacancies and interstitials to annihilate each other; and (3) for 0.7-MeV irradiation, the recovery of damage in the 65°K annealing stage is almost complete (95%). The simplest assumption to account for such complete recovery is annihilation of the defects. If we rule out annihilation of uncorrelated vacancies and interstitials by (2), simplicity leads us to assume that the defects are indeed close vacancy-interstitial pairs.

The rationale of those who wish to interpret the annealing stage at 65°K in terms of long-range migration is that this would reconcile what appears to be a drastic difference between the behavior of defects in two very similar crystals—germanium and silicon. Whan's work does point up an important similarity between the two—the formation of a vacancy-oxygen complex occurs at roughly the same temperature in both materials and accounts for about the same small fraction of the total number of displacement events that are expected to occur in the irradiation of both. The essential difference between germanium and silicon is that in n-type germanium a large recovery stage is observed at 65°K in the electrical and other properties,[1] whereas no comparable stage is observed in silicon. It is our belief that close pair defects are not stable in silicon at low temperature and that most displaced atoms recombine with the parent vacancy during irradiation. Only the small fraction that are liberated survive to migrate at higher temperatures to form the defect complexes that are observed. In germanium the close pairs are stable up to 65°K, when they recombine. Again only a small fraction of the pairs that are liberated are free to form complexes by migrating through the lattice.

[20] R. E. Whan, Appl. Phys. Letters **6**, 221 (1965).
[21] R. E. Whan, Phys. Rev. **140**, A690 (1965).
[22] J. E. Fischer and J. C. Corelli, J. Appl. Phys. **37**, 3287 (1966).
[23] J. W. Corbett, in *Solid State Physics*, edited by F. Seitz and D. Turnbull (Academic Press Inc., New York, 1966), Suppl. 7, Preface.

ACKNOWLEDGMENTS

The authors are grateful to J. S. Raby for technical assistance and E. E. Klontz for helpful discussions of this work.

APPENDIX

A calculation of the average energy of the carriers as a function of the pulse field follows: For this calculation, it is the energy exchange between carriers and lattice that is important, rather than the momentum exchange, which determines the mobility. We write the energy-balance equation for the carrier system in steady state,

$$\left\langle\frac{d\epsilon}{dt}\right\rangle_{\text{field}}+\left\langle\frac{d\epsilon}{dt}\right\rangle_{\text{scatt}}=0, \tag{6}$$

where the brackets indicate averages taken over the appropriate carrier distribution. The average rate of energy input per carrier may be taken from the experimental data to be

$$\left\langle\frac{d\epsilon}{dt}\right\rangle_{\text{field}}=\mu eE^2=\frac{\sigma E^2}{n}, \tag{7}$$

where μ, σ, and n represent the mobility, conductivity, and carrier concentration, respectively, at a pulse field E, and e is the electronic charge. At fields above the conductivity maximum, $n=n_0$, the exhaustion-range carrier concentration (which may be determined by dc Hall measurements at temperatures above 30°K). $\langle d\epsilon/dt\rangle_{\rm scatt}$ represents the energy losses of the carrier system to various carrier scattering mechanisms. The highly elastic impurity scattering mechanisms are of negligible importance for energy transfer, though charged-impurity scattering strongly affects the mobility at low fields. Impact ionization provides an important energy-loss mechanism in the avalanche breakdown region below 20 V/cm, but may be neglected at fields above the conductivity maximum, where the Sb donors are fully ionized. Intravalley optical-mode scattering and intervalley acoustic-mode scattering have relaxation times of the same form[24] and involve emission of phonons of comparable energy. If the field is applied in a (100) direction, differential heating of the electrons in different valleys can be avoided and these two mechanisms may be lumped together as "optical-mode scattering."

Conwell has calculated the lattice-scattering terms assuming a Maxwellian carrier distribution characterized by a temperature T_e.[25] Using the expression for the normal carrier mobility attributable to acoustic-mode scattering, and making straightforward approximations valid when $kT_e < k\theta$, the energy of the optical phonon, her expressions for the losses to the acoustic and optical modes may be put in the forms

$$\left\langle\frac{d\epsilon}{dt}\right\rangle_{\rm ac}=-\frac{32}{3\pi}\frac{ec^2}{(\mu_{\rm ac}T_L{}^{3/2})}T_e{}^{3/2}\left(1-\frac{T_L}{T_e}\right), \quad (8)$$

$$\left\langle\frac{d\epsilon}{dt}\right\rangle_{\rm op}=-\frac{2}{3\pi}\frac{ec^2}{(\mu_{\rm ac}T_L{}^{3/2})}\left(\frac{E_{\rm op}}{E_{\rm ac}}\right)^2\frac{k\theta}{m^*c^2}\frac{\theta^2}{(T_e)^{1/2}} \times\exp\left(-\frac{\theta}{2T_e}\right)K_1\left(\frac{\theta}{2T_e}\right), \quad (9)$$

where $\mu_{\rm ac}$ is the contribution of the acoustic modes to the normal carrier mobility, c is the speed of sound, m^* is the effective mass of the carriers, $k\theta$ is the energy, assumed constant, of the optical-mode phonon, $(E_{\rm op}/E_{\rm ac})$ is the ratio of the optical- and acoustic-mode matrix elements as defined by Conwell, and $K_1(x)$ is the modified Bessel function of the second kind.

$\langle d\epsilon/dt\rangle_{\rm ac}$ was calculated for the case of equipartition of energy among the lattice modes with which the carriers interact, but it remains valid for carrier temperatures where equipartition does not hold.[26] It is also assumed that $d\epsilon/\epsilon \ll 1$, where ϵ is the carrier energy and $d\epsilon$ is the change in energy in a carrier-phonon interaction. This assumption restricts the derivation's validity to carrier temperatures $\gtrsim 30$°K. The assumption of a Maxwellian carrier distribution is questionable, but receives some support from the estimates by Stratton[27] that indicate that in n-type germanium carrier-carrier scattering enforces a Maxwellian energy distribution for carrier concentrations above a critical value of approximately 2×10^{14} $(T_e/296)^2$ cm^{-3}. Our samples meet this criterion for values of $T_e \lesssim 200$°K. Since the carriers transfer energy among themselves much more efficiently than it is transferred in other scattering events, but transfer momentum at a comparable rate, the momentum distribution is readily predictable only for a much higher carrier concentration than is present in these samples.

Taking $\mu_{\rm ac}=(2.83\times10^7)T_L{}^{3/2}$ cm^2/V sec,[28] $\theta=400$°K, $m^*=0.22$ m_0,[7] $c=5.46\times10^5$ cm/sec, and values of $(E_{\rm op}/E_{\rm ac})^2$ of 0.3 and 0.54 that bracket the values assumed by various workers,[5,7] the energy-loss rates were calculated. The carrier temperature as a function of the field, calculated using the conductivity curve of Fig. 2 and the energy losses of Eqs. (8) and (9), is shown in Fig. 3. The upper and lower curves correspond to values of $(E_{\rm op}/E_{\rm ac})^2=0.3$ and 0.54, respectively. An independent method of estimating the carrier temperature, based on changes in the charged-impurity scattering after irradiation, was suggested in a previous paper.[29] The difficulties involved in interpreting hot-carrier mobility curves seriously limits its accuracy.

[24] C. Herring, Bell System Tech. J. 34, 237 (1955).

[25] E. Conwell, Phys. Chem. Solids 8, 234 (1959). The published expression for energy losses to optical-mode scattering should be multiplied by a factor $\exp(+\theta/2T_e)$; it is our understanding that the omission occurred during publication.

[26] D. M. Brown, Ph.D. thesis, Purdue University, 1961 (unpublished).

[27] R. Stratton, Proc. Roy. Soc. (London) **A242**, 355 (1957).

[28] E. G. S. Paige, Ref. 5, p. 96.

[29] T. A. Callcott and J. W. MacKay, *7th International Conference on the Physics of Semiconductors: Radiation Damage in Semiconductors* (Dunod Cie., Paris, 1965), Vol. 3, p. 27.